



**POLITECNICO**  
MILANO 1863

**RE.PUBLIC@POLIMI**

Research Publications at Politecnico di Milano

## Post-Print

This is the accepted version of:

D. Cutajar, A. Magro, J. Borg, K. Zarb Adami, G. Bianchi, C. Bortolotti, A. Cattani, F. Fiocchi, L. Lama, A. Maccaferri, A. Mattana, M. Morsiani, G. Naldi, F. Perini, G. Pupillo, M. Roma, S. Rusticelli, M. Schiaffino, P. Di Lizia, M. Losacco, M. Massari, M. Reali, W. Villadei  
*A Real-Time Space Debris Detection System for BIRALES*  
JBIS - Journal of the British Interplanetary Society, Vol. 72, N. 3, 2019, p. 102-108

**When citing this work, cite the original published paper.**

Permanent link to this version

<http://hdl.handle.net/11311/1092975>

## A real-time space debris detection system for BIRALES

D. Cutajar<sup>a\*</sup>, A. Magro<sup>a</sup>, J. Borg<sup>a</sup>, K. Zarb Adami<sup>a,b</sup>, G. Bianchi<sup>c</sup>, C. Bortolotti<sup>c</sup>, A. Cattani<sup>c</sup>, F. Fiocchi<sup>c</sup>, L. Lama<sup>c</sup>, A. Maccaferri<sup>c</sup>, A. Mattana<sup>c</sup>, M. Morsiani<sup>c</sup>, G. Naldi<sup>c</sup>, F. Perini<sup>c</sup>, G. Pupillo<sup>c</sup>, M. Roma<sup>c</sup>, S. Rusticelli<sup>c</sup>, M. Schiaffino<sup>c</sup>, P. Di Lizia<sup>d</sup>, M. Losacco<sup>d</sup>, M. Massari<sup>d</sup>, M. Reali<sup>e</sup>, and W. Villadei<sup>e</sup>

<sup>a</sup> Institute of Space Sciences and Astronomy (ISSA), University of Malta,  
[{denis.cutajar}{alessio.magro}{josef.borg.11}@um.edu.mt](mailto:{denis.cutajar}{alessio.magro}{josef.borg.11}@um.edu.mt)

<sup>b</sup> Dept. of Physics, University of Oxford, Oxford, OX1 3RH, United Kingdom, [kristian.zarb-adami@um.edu.mt](mailto:kristian.zarb-adami@um.edu.mt)

<sup>c</sup> Istituto Nazionale di Astrofisica - Istituto di Radioastronomia, Via P. Gobetti 101 - 40129 Bologna, Italy,  
+39 051 6965827, [g.bianchi@ira.inaf.it](mailto:g.bianchi@ira.inaf.it)

<sup>d</sup> Department of Aerospace Science and Technology, Politecnico di Milano, Via G. La Masa 34 - 20156 Milano, Italy, +39 02 23998370, [pierluigi.dilizia@polimi.it](mailto:pierluigi.dilizia@polimi.it)

<sup>e</sup> Italian Air Staff – ITAF, Viale dell’Università 4, 00185 Rome, Italy,  
[{marco.reali}{walter.villadei}@aeronautica.difesa.it](mailto:{marco.reali}{walter.villadei}@aeronautica.difesa.it)

\* Corresponding Author

### Abstract

The ever increasing satellite population in near-Earth orbit has made the monitoring and tracking of cooperative and non-cooperative objects ever more important. Non-cooperative objects, or space debris, pose a threat to existing and future satellites as they cannot avoid potential collisions. Furthermore, the orbit of the smaller debris is often not actively monitored. As the population grows, the risk of a collision increases. Thus, various institutions around the world have been upgrading their space detection capabilities in order to better monitor the objects orbiting Earth down to a few centimetres in diameter. One of the latest such systems is the BIstatic RAdar for LEo Survey (BIRALE) space debris detection system based in Italy. The BIRALE system is a bistatic radar composed of a radio transmitter in Sardinia and the Medicina Northern Cross radio telescope near Bologna as the receiver. The backend of this system includes a digital beamformer able to synthesize 32 beams covering the instrument’s Field of View (FoV). As a high-velocity object transits, its Doppler shift signature (or track) can be measured. Whilst a number of streak detection algorithms have been proposed for optical telescopes, the number of detection algorithms for high-speed objects for bistatic radars is limited. This work describes the detection algorithm used in the BIRALE space debris detection pipeline. The detection algorithm takes the beamformed, channelized data as input. Firstly, the data undergoes a number of pre-processing stages before the potential space debris candidates are identified. Secondly, the candidates are validated against a number of criteria in order to improve the detection quality. The algorithm was designed to process the incoming data across 32 beams in real-time. Initial validation results on known objects are positive and the system has been shown to reliably determine orbiting objects with minimal false positives.

**Keywords:** orbital debris, radar, detection, clustering

### 1. Introduction

Satellites have become indispensable to many areas and disciplines including telecommunications, climate research, navigation and human space exploration. Of the thousands of satellites that were put in orbit, only a fraction remain operational either due to a planned decommission or a fatal break-up. In addition, Klinkrad [1] mentions several other sources of inoperative hardware within the space environment including spacecraft used to place the satellites in orbit, such as rocket bodies, dust particles and leaked cooling agents. Collectively, these objects are often referred to as orbital or space debris. Both natural and man-made

space debris pose a considerable threat to the active satellites and space missions. As the number of space debris objects increase, the likelihood of a collision is also increased.

The increasing risk of orbit collisions has led to a heavy investment in new preventive measures to mitigate the proliferation of space debris and minimize the collision risks for active satellites. Bonnal and McKnight [2] list a number of direct removal techniques that have been proposed throughout the years. Furthermore, post-mission disposal and mitigation strategies are now taken into account during the mission design of new satellites.

It is thus important to characterize the orbital environment of Resident Space Objects (RSO) through direct observations. Measurements provide the space agencies and satellite operators with a deeper understanding of the current environment, including growth trends [3] and accumulation regions. This data is required not only at a mission design phase, but also to assess the risk of potential collisions by predicting the debris trajectory [4].

Space agencies amalgamate the output of different sensors in order to detect, track and identify both known and unknown orbiting objects. At present, the space environment is determined through both space-borne [5] and ground based optical and radar systems. Observational facilities and space surveillance networks monitor only a fraction of the space debris population. Thus, the introduction of new high sensitivity instrumentation is paramount to the better characterization of the space environment. Apart from building new high sensitivity instruments, one of the research missions of the ESA's Space Situational Awareness (SSA) goals is to use existing systems and upgrade them for the monitoring of orbital debris.

Since 2006, the Istituto Nazionale di Astrofisica (INAF), funded by the Italian Space Agency (ASI), has been investigating a number of possible radar setups at the Medicina radio astronomical station. A review of the Italian space debris activity can be found in [6] and [7]. In 2007, the Medicina 32 m parabolic antenna was used in three space debris detection tests. The observation campaigns were done in bi-static mode with the Medicina parabolic dish acting as receiver and the RT-70 parabola in Evpatoria, Ukraine, acting as transmitter. The system has been shown to be capable of detecting small sized debris in Low Earth Orbit (LEO) and Medium Earth Orbit (MEO) [8].

In 2015, INAF, in collaboration with the University of Malta and the Politecnico di Milano, embarked on an ambitious project to upgrade one of INAF radio telescopes for use in SSA. The aim of the project is the design and implementation of an operational bistatic radar for orbital debris in LEO as part of the European Space Surveillance & Tracking (SST) Support Framework [9] [10].

This contribution describes the processes used in the detection of orbital objects with the BIRALES system. First, an overview of the radar system is given. This is followed by a description of the data processing software implemented to process the incoming data. Finally, the detection processing pipeline is presented

together with some preliminary results of this novel system.

## 2. BIRALES: A Bi-static radar for space debris detection

The BIRALES is a bistatic radar which makes use of the Radio Frequency Transmitter (TRF) located in the Italian Joint Test Range of Salto di Quirra (PISQ), in Sardinia as a transmitter operating in continuous wave mode with a maximum output power of 10kW. The Basic Element for SKA Training (BEST) [11], located at the Medicina radio astronomical station, near Bologna, Italy, is used as receiving component of the bistatic radar.

The BEST project was a series of planned upgrades to a subset of the Northern Cross antenna. The array is currently at the second stage of the project called the BEST2 (Fig 1.) [12]. It consists of eight East-West oriented cylindrical concentrators as shown in Figure 1. Each cylinder has a reflecting surface made of 430 parallel steel wires of 0.5 mm placed 2 cm apart [13].



Fig. 1. The BEST2 array within the Northern Cross in Medicina, near Bologna, Italy.

Four low noise receivers are installed on the focal line of each cylinder. Each receiver combines the dipole signals in groups of 16, resulting in four analogue channels per cylinder. This gives a total of 32 elements which are arranged in a 4 by 8 grid having a total collecting area of  $1420 \text{ m}^2$ .

The amplified RF signals travel to a receiver room, located within the central building, through analogue optical fibre links 500 m long. The signals are down converted to the intermediate 30 MHz frequency and then fed to a ROACH-based digital backend developed by [14] [15]. The signals are digitized and channelized

into 1024 single polarisation, 78.125 kHz wide, coarse frequency channels.

The channelized data are transferred as a UDP stream to a processing server over a 10 GBit link [16]. At the processing server, a purpose-built space debris software backend analyses the incoming data for radar echoes reflected off in-orbit objects.

### 3. A data processing backend for space debris: PyBirales

The data processing system, called PyBirales, processes the incoming data from the BEST2 digital backend in real-time. The data rate of the instrument is in the order of tens of megabytes per second. For this reason, PyBirales was developed in Python whilst computationally intensive tasks were developed in C++ and imported into Python.

The incoming antenna signals are processed using the PyBirales data processing pipelines. A data processing pipeline is made up of a chain of separate processing stages as shown in Figure 2. At each processing stage, or module, the incoming data is mutated and passed over to the next processing stage.

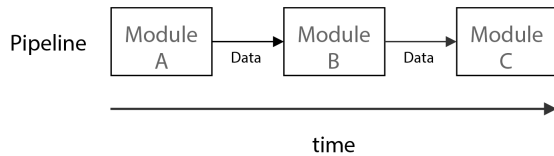


Fig. 2. The pipeline design pattern used in the PyBirales pipelining framework

The processing modules can be chained in any order, so long as the data container, or data blob, transferred to the subsequent module is compatible. A check on blob compatibility in-between the chained modules is performed upon the initialisation of the pipeline.

The processing pipelines in PyBirales are designed to process the data in real-time. This means that the following real-time condition in each module is met,

$$\text{time taken} < \frac{\text{Number of Samples}}{\text{Sampling Rate}} \quad (1)$$

For instance, at a sampling rate of 78,125 samples per second, 262144 samples need to be processed in less than 3.35 s for the real-time condition to be met. This condition has to be met at each processing stage within the pipeline.

The creation of a data processing pipeline is facilitated by a framework that is able to generate different processing pipelines with ease. This framework provides a standard and concise method of chaining a set of modules into a pipeline by making use of a pipeline manager that initialises the processing modules and chains one processing module to the next. Using this system, a number of pipelines can be created, such as the detection and the correlation pipelines. The latter is an integral part of the calibration routine that is used to calibrate the BEST2 array.

#### 3.1 Calibration

A radio interferometer array will always be liable to geometrical and instrumental delays, with the latter changing on short time scales and thus requiring frequent corrections. Geometrical delays arise from the fact that the array itself is inherently composed of antennas with a quantified ground separation, with radio waves arriving at each antenna at specific time delays. Such introduced delays can thus be easily defined and corrected for with accurate knowledge of the antenna and the observed point source. On the other hand, instrumental delays are less predictable and are inherent to the instrument itself. Such errors are the reason for which the calibration observation of a point source passing through the beam is necessary.

For calibration of the BEST2 array, a correlation matrix of complex visibilities is first produced by the correlation pipeline. This is generated through an observation of an unresolved calibration source, such as Cassiopeia A or Taurus A, as it transits through the field of view of the array's beam. Consequently, after the point source transits at the meridian through the beam, the entire correlation matrix dataset is inspected by the calibration routine. The selection of those visibilities obtained at the point source's exact moment of passage at the meridian ensues. These visibilities are selected on the premise that, for a perfectly calibrated array, the phase component of the complex visibilities for all baselines during the passage of a point source at zenith should be equivalent to zero. Corrections to obtain such visibilities' phases are calculated for every antenna, taking a specific antenna as phase reference.

Thus, after obtaining phase coefficients through this routine, the visibilities are phase aligned accordingly. A gain calibration routine follows, using the phase calibrated visibilities as a starting point. The gain calibration assumes that the source power observed is equal throughout the array, with its absolute value dependent only on the source brightness itself. A logarithmic implementation of a least squares estimation technique is used for obtaining an estimate for gain

solutions per antenna. These are combined with the calibration coefficients obtained from the initial phase calibration routine (which themselves also solve for gain errors to some extent) in order to obtain the final calibration coefficients. Such coefficients are normally produced once per observation.

The complexity of the system is shielded away from the operator by a web-application. This is a consolidated approach in monitoring, control and administration of PyBirales. Ultimately, the goal of the system was to build the necessary components that will eventually be used for the detection of orbital debris. The next section gives an in-depth description of the detection pipeline within PyBirales, and how this is used for the detection of orbital debris in LEO.

#### 4. Detection strategy

The detection of RSO objects is done through a dedicated detection pipeline built using the PyBirales framework described earlier. The detection pipeline makes use of a number of processing modules and its composition is illustrated graphically in Figure 3.

The incoming data from the digital backend is consumed by the receiver module. The signals from the 32 antennas in the BEST2 array are beam formed into a number of beams. The number of beams generated, together with their pointing, is configurable and can be specified by the operator of the PyBirales software backend. At present, the default configuration generates 32 coherent beams within the primary beam of the BEST2 array.

The channel bandwidth is too wide for the detection of small signature objects such as space debris. Hence, finer channelization is applied at the channelizer module. A polyphase filter bank channelizer is used since leakage is significantly less than a standard Discrete Fourier Transform. The channelizer splits a single coarse channel into 8192 separate channels of around 9.5 Hz each. This gives a temporal resolution of around 100 ms.

The output data blob of the channelizer module serves as the input to the pre-processor module. It is an n-dimensional array consisting of 8192 channels by 32 time samples for each of the 32 beams. The operations described in the following sections are applied across all the 32 beams generated by the PyBirales beamformer.

##### 3.1 Pre-processing and Filtering

The pre-processing module takes in the beam formed, channelized data blobs and calculates the power  $P$  from the received antenna voltages  $V$  as,

$$P = 10 \log_{10} V^2 \quad (2)$$

An estimate for the background noise at a channel was taken to be the root mean square value of the power of the  $N$  samples at that channel  $c$ . This noise needs to be filtered out before a detection could be made. Filtering of this data is done at the next module in the pipeline namely filtering.

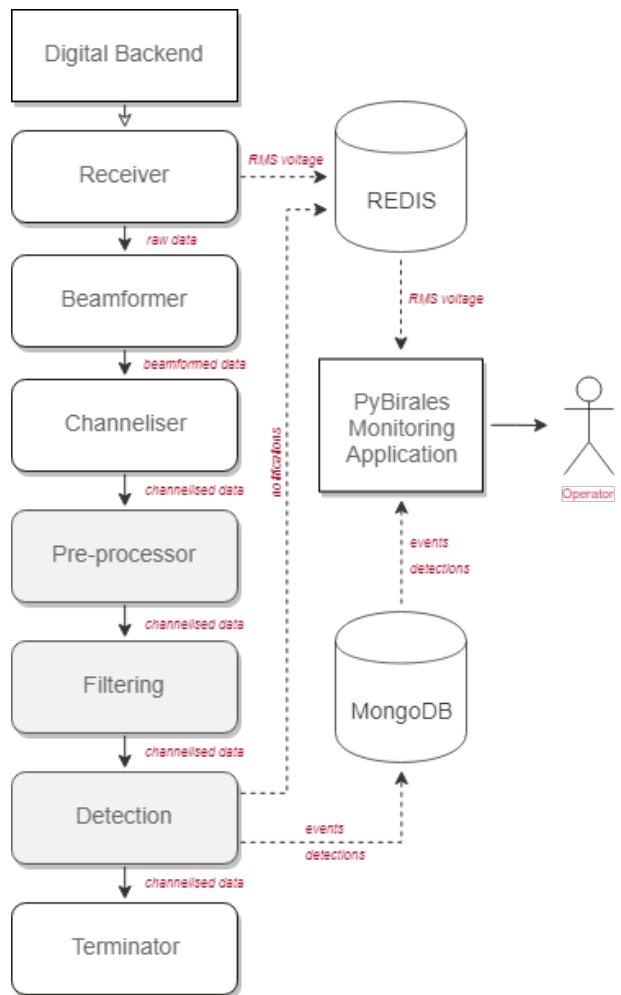


Fig. 3. A block diagram of the detection pipeline used in the BIRALEs system. The modules pertaining to the detection of RSO are highlighted in grey.

The filtering module consists of a number of filters that are applied on the data sequentially. The aim of the filters is to remove the background noise as much as possible. This process reduces the number of data points that the detection algorithm has to process thereby simplifying the detection problem at a later stage.

Figure 4 shows a subset of the raw, pre-processed data that is depictive of the input to the filtering module. One may note the radar signature of an RSO (NORAD 30774) as it passed through the FoV of the instrument. The Radio Frequency Interference (RFI) contribution of the transmitter is also visible.

The first component in the filtering module is the background noise filter. A data point is considered to be noise if its power value  $P$  is within four standard deviations,  $\sigma$  of the mean noise power  $P_\epsilon$  (Eq 3).

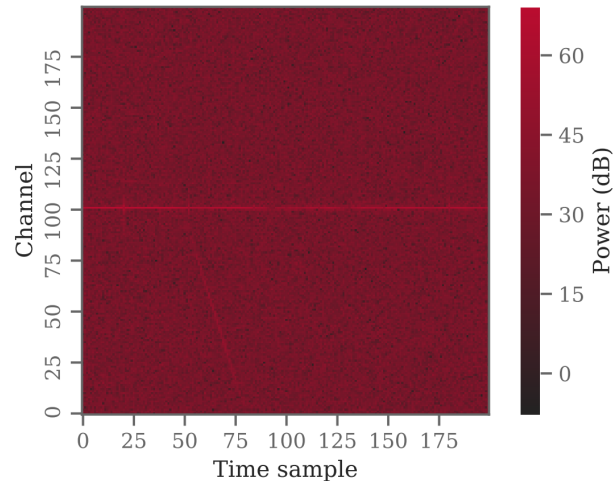


Fig. 4. A spectrogram of a subset of the channelized, pre-processed data showing the power received across a set of channels and time samples. The transmitter RFI frequency and the radar signature of an RSO object can be noted within this image.

The application of this filter clips the bulk of the data given that most of the data in this blob is noise. However, this filter does not adequately filter the RFI noise introduced by the transmitter line.

$$f(P) = \begin{cases} P, & \text{if } P \geq 4\sigma + P_\epsilon \\ 0, & \text{otherwise} \end{cases}$$

(3)

In observations where the transmitter is located near the receiving part of the radar, the RFI signature of the transmitter can be measured. This is usually distinguished by two unique characteristics. First, due to the relative proximity of the transmitter, the measured power is very high, usually orders of magnitude higher than other detected signals. Second, the transmitter frequency does not change in time and is present within the same frequency channels across time. These two features are exploited in the transmitter line filter.

The channels at which a high power is measured are identified by performing a peak search on the data. This is achieved by summing the bandpass across  $N$  samples. Channels whose summed power is greater than an arbitrary threshold  $\tau$  are considered to be peaks. At these channels, the power  $P_c$  across all time samples is clipped (Eq. 4).

$$f_{tx}(P_c) = \begin{cases} 0, & \sum_{n=0}^N P_c \geq \tau \\ P_c, & \text{otherwise} \end{cases}$$

(4)

After the application of these filters, the data is still characterized by random and isolated pixels with a high SNR. These data points, or pixels, can be removed through binary hit-or-miss transform. This transform finds the pixels which match a specified pattern or mask. The mask is a representation of a single pixel with no immediate neighbouring pixels.

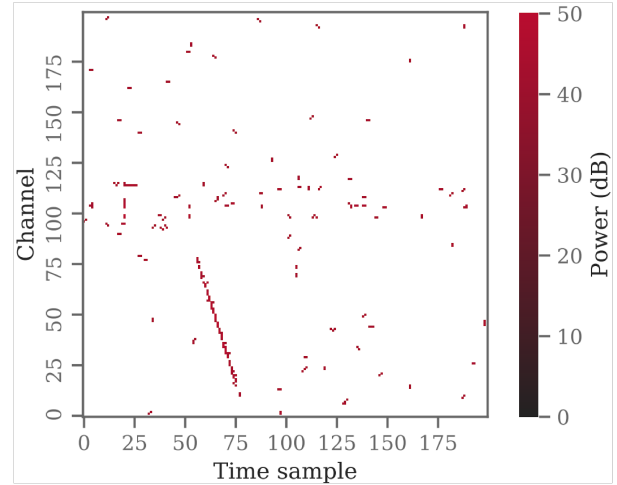


Fig. 5. The output of the filtering module after filtering the data from the background noise, transmitter RFI and speck noise. It can be noted that most of the noise is eliminated and the radar signature of the target RSO is clearly noticeable.

As shown in Figure 5, the application of the aforementioned three filters proved to be very effective in clipping most of the noise thereby reducing the complexity of the detection algorithm. However, some noise can still be present after this filtering process. Thus, the detection algorithm, needs to be robust enough to cope for any noise artefact that are left after the filtering stage.

### 3.2 Detection

The detection module accepts channelized data which has been pre-processed and filtered at the previous modules in the pipeline. The aim of the

detection algorithm is to identify the radar echoes reflected by the RSO. These echoes are characterised by a sharp increase in intensity when compared to the background level. Given the linearity of these radar signatures, classical edge detection algorithms such as Hough transforms were investigated initially. The Hough transform solves the edge detection problem by converting the problem to a local peak detection search in parameter space [17]. In earlier work [18], this method proved to be effective in the identification of large RSOs. However, the algorithm proved to be less effective in the presence of noise and targets with a low SNR.

The manuscript presents the use of a clustering technique for the automated identification of these radar echoes. Clustering is the unsupervised organisation of unlabelled data into groups called clusters. Patterns within one cluster are considered to be more similar to each other than to any other pattern associated with a different cluster [19].

Given that the number of radar echoes present is not known a priori, a hierarchical clustering technique was used. Consequently, an established, density-based clustering technique known as Density-Based Spatial Clustering of Applications with Noise (DBSCAN) [20] was used. An added advantage of this clustering algorithm is that it is able to classify isolated pixels as noise thereby distinguishing them from valid clusters.

The algorithm groups together data points based on their proximity to each other using a distance metric a minimum number of points per cluster. The  $Eps$ -neighbourhood of a point  $q$  is defined by  $N_{Eps}(q) = \{p \in D | dist(q, p) \leq Eps\}$  where,  $dist(q, p)$  is the distance function and  $Eps$  is a constant that defines the maximum distance between two data points  $p$  and  $q$  belonging to the same cluster. The  $Eps$  distance was determined empirically and set to 5 pixels.

In DBSCAN, data points are classified as either being inside (core points) or at the edge of a cluster (border points). A point  $p$  is said to be directly density-reachable from a point  $q$  if  $p \in N_{Eps}(q)$  and  $|N_{Eps}(q)| \geq MinPts$  where  $MinPts$  is the minimum number of points in a cluster. On the other hand, a point  $p$  is said to be density-reachable from a point  $q$  if there is a chain of points  $p_1, \dots, p_n, p_1 = q, p_n = p$  such that  $p_{i+1}$  is directly density-reachable from  $p_i$ . A border point can also be considered to be density-connected to a point  $q$  if there is a point  $o$  such that both  $p$  and  $q$  are density-reachable from  $o$ . Thus, a cluster  $C$  is considered to be a non-empty subset of  $D$  if the following conditions are satisfied.

Maximality:  $\forall p, q: \text{if } p \in C \text{ and } q \text{ is density-reachable from } p \text{ w.r.t. } Eps \text{ and } MinPts, \text{ then } q \in C$ .

Connectivity:  $\forall p, q: \text{if } p \in C \text{ and } q \text{ is density-connected to } q \text{ w.r.t. } Eps \text{ and } MinPts$ .

Points which do not satisfy these conditions are regarded as noise such that if  $C_1, \dots, C_k$  are clusters of  $D$ , then noise =  $\{p \in D | \forall i: p \notin C_i\}$ . Once the point  $p$  is classified as either a *core*, border or noise, the algorithm moves to the next point in  $D$ . Thus, this approach groups points that are closely packed together, expands clusters in any direction where there are nearby points using a density-based metric. This way, it is able to deal with different shapes of clusters making it ideal for the detection of radar echoes.

The clusters identified by this algorithm are referred to be beam tracklets or just tracklets. A tracklet is a grouping of pixels in a beam with an associated Doppler shift, channel and time epoch. Figure 6, shows the clusters labelled by the DBSCAN for a typical dataset. One may observe that the algorithm is very effective in grouping most of the pixels related to the target detection. Isolated, small, clusters of pixels are also correctly classified as noise. However, one may also observe the presence of clusters which are clearly false positives. This is especially true near the channels at which the transmitter RFI frequency was present.

False positives are handled by a validation process on the detected clusters. The validation process consists of a number of criteria. For instance, clusters made up of a few data points are ignored. Furthermore, the shape of the cluster is also taken into account. Tracklets are expected to be linear where the frequency and time of a detection are strongly correlated.

Another optimisation that was introduced was to ignore clusters with an unrealistic Doppler shift value. Analysis of the catalogued objects in orbit put the expected Doppler shift  $\Delta f$  to lie between -12143 and +13245 Hz. Clusters with a Doppler shift value outside of this range were dropped. Similarly, a range for the rate of change in the Doppler shift of the detection was obtained. The rate of change in the measured Doppler is expected to lie between -291.47 and -69.62 Hz s<sup>-1</sup>. This process ensures that only valid RSO tracklets are passed on to the next stage.

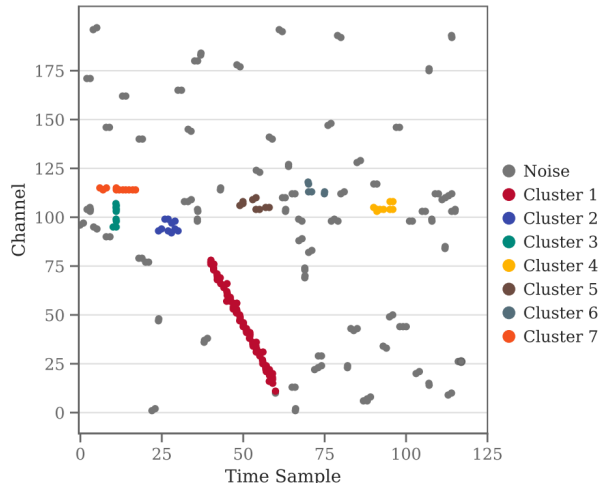


Fig. 6. The output of the DBSCAN algorithm that is applied on the filtered data. The target object is identified as being Cluster 1. False positives are also identified including data points identified as Noise.

A single RSO transient can produce multiple tracklets across multiple beams. These tracklets can appertain to the same radar echo, or track, of an RSO. A track can span multiple data blobs. As a result, different tracklets in subsequent data blobs can belong to the same RSO track. Thus, a system of merging, or linking, these tracklets, across multiple beams and blobs, belonging to the same RSO was put in place. This process is called tracklet linking.

In tracklet linking, the detection tracklets are associated with a single RSO track or just track. This is achieved by comparing the parameters of the detection tracklets with the RSO tracks. A RSO is associated with a parent RSO track if the cosine similarity between the two is below a threshold. In so doing, the track grows as new tracklets are detected and associated with it. In the case when no track exist in the queue, an empty RSO track is created and the new cluster is associated with it.

The track is kept in memory in order to be able to compare the track with any future detections of new tracklets. The candidate is popped out of the queue when the candidate is not updated for a specified number of iterations. This ensures that no two tracks belonging to two distinct RSO get merged by chance. Whilst this approach is adequate, a more accurate approach is to calculate the theoretical time at which the space candidate exists the instrument FoV.

RSO tracks which were created or modified during an iteration are persisted to the MongoDB database. The detected RSO tracks and other observation details are made available to an operator in real-time through the monitoring dashboard that is shipped with PyBirales. At

the end of an observation, the detection made are saved in TDM format at a post-processing stage once the pipeline is stopped.

This TDM file is also the input to the orbital determination block developed by a team of researchers at the Politecnico di Milano, Italy [4]. The tailored algorithm makes use of the beam illumination sequence, SNR and Doppler shift together with the beam distribution and antenna pointing. These parameters are used to refine the orbital parameters of known RSO or perform a preliminary orbit determination in the case of unknown objects.

## 5. Results and Discussion

One of the earliest tests of the BIRALES system was performed on the 30<sup>th</sup> of June 2017 observation, in which the system successful in detecting the OSCAR 16 (PACSAT) (NORAD 20439). Launched in January 1990, OSCAR 16 is an operational satellite for the amateur radio community. Having a RCS of 0.1139 m<sup>2</sup>, is an ideal target to test the system capability thus far. The parameters of the observation are listed in Table 1.

Table 1. The parameters for the NORAD 20439 observation campaign on 30<sup>th</sup> June, 2017

Transit time (UTC)	2017-06-30 12:13:46.043
TRF Elevation (°)	72.150251
TRF Azimuth (°)	120.76353
BEST2 Declination (°)	29.988066
Altitude (km)	786.75898
TRF Range (km)	821.32114
BEST2 Range (km)	1054.9398
Slant Range (km)	1876.2609
RCS (m <sup>2</sup> )	0.1143
Doppler shift (Hz)	+8192.5523

The measured SNR profile of the detected object is shown in Figure 7. Multiple beams are illuminated as the object passes through the instrument's FoV. The Doppler profile of this detection is represented in Figure 8. In this case, the highest SNR per time epoch is selected. One may observe that a strong linear relationship with a correlation coefficient of -0.99985 obtained, indicative of a hyper-velocity transient.

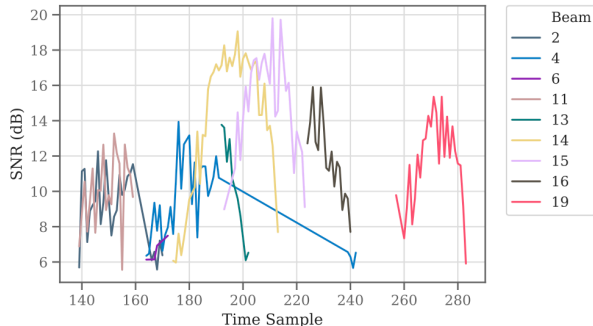


Fig. 7. A plot of power against time for the NORAD 20439 detected on the 30<sup>th</sup> of June 2017

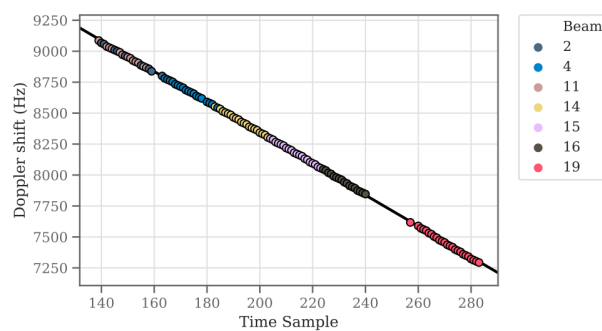


Fig. 8. A Doppler profile for the NORAD 20439 detected on the 30<sup>th</sup> of June 2017.

A global SNR maximum of 19.795 dB was measured in the central beam at 12:13:45.869 at a Doppler shift of 8208.770 Hz. Comparing these values with the expected values in Table 1 one finds that the transit time is off by less than half a second. The measured Doppler shift shows a similar level of agreement.

## 6. Conclusion

With the exponential increase in satellite launches, the population of defunct of broken material in space has grown substantially. This is especially true in sensitive orbits such as the LEO and GEO regimes. These material, collectively known as space debris, can pose a considerable threat to the operational satellites. This makes the monitoring of these objects of the utmost importance.

In this work, a new process for the detection of high velocity RSO is presented. The detection process makes use of new data processing software that was especially built to process the incoming data from the BEST2 digital backend at the Medicina radio astronomical station.

The detection module uses a clustering algorithm, DBSCAN, to group neighbouring pixels into detection

clusters or tracklets. These detection tracklets are validated against a number of criteria and grouped into RSO tracks. Space debris tracks are saved to a database and made available to the real-time monitoring front-end that is shipped in PyBirales. Detection information can also be dumped to disk and made accessible to the orbital determination block within the BIRALE project.

Preliminary results indicate that the BIRALE system is able to detect objects at an RCS of  $0.11 \text{ m}^2$  at a slant range of 1876 km. These initial results are encouraging and will be extended in future works. For instance, the data processing system will be optimised to accommodate a higher data rate in an eventual upgrade of the BEST2 system. Furthermore, tests on smaller objects in beam park experiments are planned. In these observations, the performance of other detection strategies may be compared to the one presented in this work. Apart from establishing the sensitivity of this novel system, these observation test the reliability of this new radar system within the European SST network.

## Acknowledgements

The research activities and operations described in this work was developed thanks to the funding from the European Commission Framework Programme H2020 and Copernicus, “SST – Space Surveillance and Tracking” contract No. 785257-2-3SST2016 and No. 237/G/GRO/COPE/16/8935-1SST2016.

The Northern Cross Radio Telescope is a facility of the University of Bologna operated under agreement by the IRA-INAF (Radio Astronomy Institute – National Institute of AstroPhysics).

## References

- [1] H. Klinkrad. Space debris. Springer, 2006, pp. 5–57.
- [2] C. Bonnal and Darren S. McKnight. IAA Situation Report on Space Debris. Tech. rep. International Academy of Astronautics (IAA), 2016, p. 169.
- [3] S. Montebugnoli et al. “The bistatic radar capabilities of the Medicina radiotelescopes in space debris detection and tracking”. In: Advances in Space Research 45.5 (2010), pp. 676–682.
- [4] P. Di Lizia et al. “Performance assessment of the multibeam radar sensor birales for space surveillance and tracking”. In: Proceedings of 7th European Conference on Space Debris. 2017.
- [5] M. Grassi, E. Cetin, and A. G. Dempster. “Enabling orbit determination of space debris using narrowband radar”. In: IEEE Transactions on

- Aerospace and Electronic Systems 51.2 (2015), pp. 1231–1240.
- [6] F. Piergentili et al. “Italian activity in space debris measurements”. In: Fifth European Conference on Space Debris. Vol. 672. 2009.
- [7] G. Pupillo et al. “The INAF contribution to the ASI Space Debris program: observational activities.” In: Memorie della Societa Astronomica Italiana Supplementi 20 (2012), p. 43.
- [8] G. Pupillo et al. “Space debris radar experiments at the medicina VLBI dish”. In: European Space Agency, (Special Publication) ESA SP 672 SP.April (2009), pp. 2–5. issn: 03796566.
- [9] Decision. Establishing a Framework for Space Surveillance and Tracking Support no 541/2014/EU.
- [10] A. Morselli et al. “A new high sensitivity radar sensor for space debris detection and accurate orbit determination”. In: 2015 IEEE Metrology for Aerospace (MetroAeroSpace). June 2015, pp. 562–567.
- [11] S. Montebugnoli et al. “Italian SKA test bed based on cylindrical antennas”. In: Astronomische Nachrichten: Astronomical Notes 327.5-6 (2006), pp. 624–625.
- [12] S. Montebugnoli et al. “BEST: basic element for SKA training”. In: Wide Field Astronomy & Technology for the Square Kilometre Array. 2009.
- [13] P. Bolli et al. “Basic element for square kilometer array training (BEST): Evaluation of the antenna noise temperature”. In: IEEE Antennas and Propagation Magazine 50.2 (2008), pp. 58–65.
- [14] G. Foster et al. “Implementation of a direct-imaging and FX correlator for the BEST-2 array”. In: Monthly Notices of the Royal Astronomical Society 439.3 (2014), pp. 3180–3188.
- [15] F. Perini et al. “Skads”. In: First MCCT-SKADS Training School. Vol. 59. SISSA Medialab. 2008, p. 008.
- [16] A. Magro, J. Hickish, and K. Z. Adami. “Multibeam Gpu Transient Pipeline for the Medicina Best-2 Array”. In: Journal of Astronomical Instrumentation 02.01 (2013), p. 1350008.
- [17] J. Illingworth and J. Kittler. “A survey of the Hough transform”. In: Computer vision, graphics, and image processing 44.1 (1988), pp. 87–116.
- [18] A. Morselli et al. “Orbit Determination of Space Debris Using a Bi-Static Radar Configuration with a Multiple-Beam Receiver”. In: Proceedings of the International Astronautical Congress, IAC (2014), pp. 1–11. issn: 00741795.
- [19] A. K Jain, M Narasimha Murty, and Patrick J Flynn. “Data clustering: a review”. In: ACM computing surveys (CSUR) 31.3 (1999), pp. 264–323.
- [20] M. Ester et al. “A density-based algorithm for discovering clusters in large spatial databases with noise.” In: AAAI. 1996.